Enhanced Energy and Quantum Efficiencies of a Nanocrystalline Photoelectrochemical Cell Sensitized with a Donor−Acceptor Dyad Derived from Fluorescein

Shigeki Hattori,[†,‡] Taku Hasobe,[†,‡] Kei Ohkubo,[†,‡] Yasuteru Urano,[§] Naoki Umezawa,[§] Tetsuo Nagano,[*,§] Yuji Wada,[†] Shozo Yanagida,[*,†] and Shunichi Fukuzumi[*,†,‡]

Department of Material and Life Science, Graduate School of Engineering, Osaka University, Suita, Osaka 565-0871, Japan, CREST, Japan Science and Technology Agency, Suita, Osaka 565-0871, Japan, and Graduate School of Pharmaceutical Sciences, The University of Tokyo, Bunkyo-ku, Tokyo 113-0033, Japan

Received: May 31, 2004; In Final Form: July 4, 2004

The dye-sensitized photovoltaic cells were prepared by using donor−acceptor dyads derived from fluorescein. The photovoltaic measurements were performed using a standard two-electrode system consisting of a working electrode and a Pt sputtered electrode in air-saturated methoxyacetonitrile containing 0.5 M iodide and 0.05 M I_2. The xanthene dye-sensitized photovoltaic cells of the charge-separation type exhibit significant enhancement in the photoelectrochemical performance as compared with those of fluorescein without the charge-separation unit. The overall power conversion efficiency ($\eta = 1.6\%$) has been attained by using a fluorescein derivative composed of an electron donor (diphenylanthracene) unit and an acceptor unit (difluoroxanthene), assembled on a $ZnO-SnO_2$ composite film as an oxide semiconductor.

Introduction

Fluorescein derivatives have been widely employed to develop useful fluorescence probes for important biomolecules, such as nitric oxide and calcium ion, since fluorescence imaging is the most powerful technique currently available for continuous observation of the dynamic intracellular events of living cells.[1−5] The fluorescence quantum yields of fluorescein derivatives can be controlled by photoinduced electron transfer from the electron donor moiety to the singlet excited state of the xanthene moiety.[4,5] The occurrence of photoinduced charge separation has been demonstrated using a number of fluorescein-based probes in which the electron donor moiety is directly linked with the xanthene moiety.[5] Fluorescein derivatives have also been used as suitable dyes to study interfacial electron transfer in dye-sensitized solar cells (so-called Grätzel type dye-sensitized solar cell; DSSC).[6−14] The role of the dye molecule in light−energy conversion is to act as an antenna which captures the energy of sunlight, initiating ultrafast electron injection from the singlet excited state of the dye into the conduction band of the semiconductor in the femtosecond time domain.[12,13]

On the other hand, the photoinduced charge separation is the key step in the natural photosynthetic reaction center.[15] Extensive efforts have so far been devoted to design and synthesize electron donor−acceptor linked molecules to achieve efficient photoinduced charge separation.[16−23] However, fluorescein derivatives linked with an electron donor moiety, which have been commonly used as useful fluorescence probes in the biological systems (vide supra),[5] have yet to be employed as dyes in DSSC.

We report herein significant enhancement of the photoelectrochemical properties of DSSC using a series of fluorescein derivatives linked with an electron donor moiety, which afford long-lived charge-separated states upon photoexcitation of the xanthene moiety as compared with those of DSSC of the corresponding reference fluorescein derivatives without an electron donor moiety. We have previously reported the detailed photodynamics of 9-[2-(3-carboxy-9,10-diphenyl)anthryl]-6-hydroxy-3*H*-xanthen-3-one (DPAX), used as a fluorescent probe in which the diphenylanthryl group acts as an electron donor unit.[5] In this study, we used DPAX and its derivatives (**1**, **2**, and **3**) and the corresponding reference compounds (**4**, **5**, and **6**), which are shown in Figure 1. The DPAX derivatives **2** and **3** contain substituted chlorine and fluorine to control the energy level of the charge-separated state.

Experimental Section

Materials. Preparation of DPAX (**1**, **2**, and **3)** has been described elsewhere.[2b] Fluorescein derivatives (**4**, **5**, and **6**) were purchased from Sigma-Aldrich Co., Tokyo Kasei Kogyo Co., Ltd., and Molecular Probes, Inc., respectively. All solvents and chemicals were of reagent grade quality, purchased, and used without further purification unless otherwise noted.

Preparation of Dye-Sensitized Solar Cells. Nanoporous TiO_2 electrodes were prepared by dropping the colloidal suspensions of TiO_2 nanoparticles (P25, $d = 21$ nm, Nippon Aerogel) on an optically transparent electrode (OTE) (Nippon Sheet Glass, SnO_2:F, 8 Ω/square) with a glass rod and adhesive tapes as a spacer. The resulting electrodes (OTE/TiO_2) were annealed at 450 °C in air for 30 min. The thickness of the electrodes ranged between 13 and 14 μm, as measured by a profiler.

Nanoporous $ZnO-SnO_2$ electrodes were prepared by the following procedure.[24,25] A colloidal 15% aqueous dispersion of SnO_2 (Alpha Chemicals) of crystallite size ∼0.015 μm (3.0 mL), acetic acid (0.1 mL), and ZnO of crystallite size ∼0.5 μm (0.6 g) were ground in an agate mortar, mixed with 7 mL of a methanol−water (1:1) mixture, and agitated for 10 min. The dispersion was then sprayed onto an OTE (OTE/$ZnO-SnO_2$),

* Authors to whom correspondence should be addressed. E-mail: fukuzumi@ap.chem.eng.osaka-u.ac.jp (S.F.).
† Osaka University.
‡ Japan Science and Technology Agency.
§ The University of Tokyo.

10.1021/jp047656p CCC: $27.50
Published on Web 08/31/2004

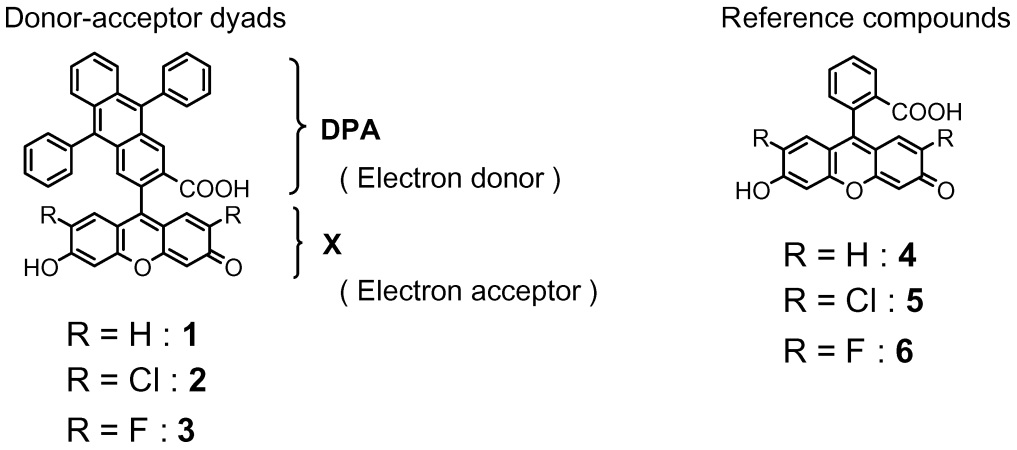

Figure 1. Structures of DPAX and reference compounds used in this study.

and the resulting electrodes were annealed at 450 °C in air for 30 min. The thickness of the electrodes ranged between 13 and 14 μm, as measured by a profiler.

Coloration of the oxide semiconductor surface with the dye was carried out by immersing the film (still warm, i.e., ~80−100 °C) for 12 h in a *tert*-butyl alcohol−acetonitrile (1:1) mixture containing 3.0×10^{-4} M of the dye. After completion of the dye adsorption, the electrode was withdrawn from the solution, washed with acetonitrile, and dried. Additionally, after the dye-coated film was immersed in 0.1 M NaOH aq solution overnight, the dye was desorbed from the film into solution, which was used to determine the amount of dye molecules adsorbed onto the film by measuring the absorbance. The UV−visible spectra were recorded on a Shimadzu 3100 spectrophotometer. Fluorescence measurements of DPAX derivatives were performed on a Shimadzu RF-5000 spectrofluorophotometer.

Electrochemical Measurements. Electrochemical measurements were performed on a BAS 100 W electrochemical analyzer in deaerated 0.1 M NaOH aq solution containing 5×10^{-3} M Na_2SO_4 as supporting electrolyte at 298 K. A conventional three-electrode cell was used with a platinum working electrode (surface area of 0.3 mm^2) and a platinum wire used as the counter electrode. The glassy carbon working electrode was polished with BAS polishing alumina suspension and rinsed with acetone before use. The counter electrode was a platinum wire. The measured potentials were recorded with respect to an Ag/AgCl (saturated KCl) reference electrode.

Photoelectrochemical Measurements. Photocurrent−voltage characteristics of solar cells were measured using a voltage−current source monitor (Advantest R6246) under AM1.5 simulated light source (Yamashita Denso, YSS-80). Incident photon-to-photocurrent efficiency (IPCE) measurements were carried out using a setup for IPCE measurements (PV-25DYE, JASCO) under 5 mW/cm^2 monochromatic light illuminations. Solar cells were made by placing the Pt sputtered optically transparent electrode (F-doped SnO_2 sheet resistance 10 Ω/square, Asahi Glass) on the dye-coated semiconductor film, and then the electrolyte was introduced from the edge of the two glass substrates just before the measurements.

Theoretical Calculations. Density-functional theory (DFT) calculations were performed on a COMPAQ DS20E computer. Geometry optimizations were carried out using the Becke3LYP functional and the 6-31G* basis set,[26,27] with the restricted Hartree−Fock (RHF) formalism, as implemented in the Gaussian 98 program.[28] Graphical output of the computational results were generated with the Cerius^2 software program developed by Molecular Simulations, Inc.

TABLE 1: Number of Dye Molecules Adsorbed on TiO_2 or ZnO−SnO_2 Films

	molecules/cm^2	
compound	TiO_2	ZnO−SnO_2
1	4.0×10^{15}	7.0×10^{15}
2	4.1×10^{15}	6.8×10^{15}
3	3.9×10^{15}	7.0×10^{15}
4	5.4×10^{15}	9.4×10^{15}
5	5.8×10^{15}	9.5×10^{15}
6	6.0×10^{15}	9.3×10^{15}

Results and Discussion

Absorption Properties of TiO_2 Electrodes Modified with DPAX Derivatives. DPAX derivatives were adsorbed on the oxide semiconductor surface by immersing the film in a *tert*-butyl alcohol−acetonitrile (1:1) mixture containing the dye (see Experimental Section). The dyes were desorbed with 0.1M NaOH aq solution. The number of dye molecules adsorbed on TiO_2 films was determined from the absorbance of desorbed dyes in solution using the molar absorption coefficients of dyes (for the spectral data, see Supporting Information, S1 and S2).[29] The results are summarized in Table 1. The numbers of adsorbed dye molecules of **1**−**3** are smaller than those of the reference compounds **4**−**6** because of the larger size of **1**−**3**, which contain the donor moiety, as compared with **4**−**6**.

The absorption spectra of DPAX derivatives and the corresponding reference compounds on OTE/TiO_2 are shown in Figure 2, exhibiting significant broadening as compared with those in NaOH aq solution (see Supporting Information, S1). Such broadening indicates that the molecular environment on OTE/TiO_2 is significantly perturbed because of the aggregation of the dye molecules. The absorbance of OTE/TiO_2/**1**−**3** is smaller than that of the corresponding reference electrode (OTE/TiO_2/**4**−**6**), resulting from the smaller numbers of adsorbed dye molecules of **1**−**3** than those of **4**−**6** (Table 1).

The fluorescence of DPAX (**1**) is significantly quenched by electron transfer from the diphenylanthracene-2-carboxylic acid (DPA) moiety to the singlet excited state of the xanthene moiety (X) of DPAX. The photoexcitation of the xanthene moiety of DPAX results in formation of the radical ion pair, i.e., the DPA radical cation and the xanthene radical anion, both of which were detected as the transient absorption spectra in the laser flash photolysis experiments.[5] The formation of the radical ion pair following photoexcitation of DPAX was also confirmed by the ESR detection.[5] The fluorescence quantum yields of **1**−**3** are determined as 0.007, 0.006, and 0.006, respectively, which are significantly smaller than those of the reference compounds

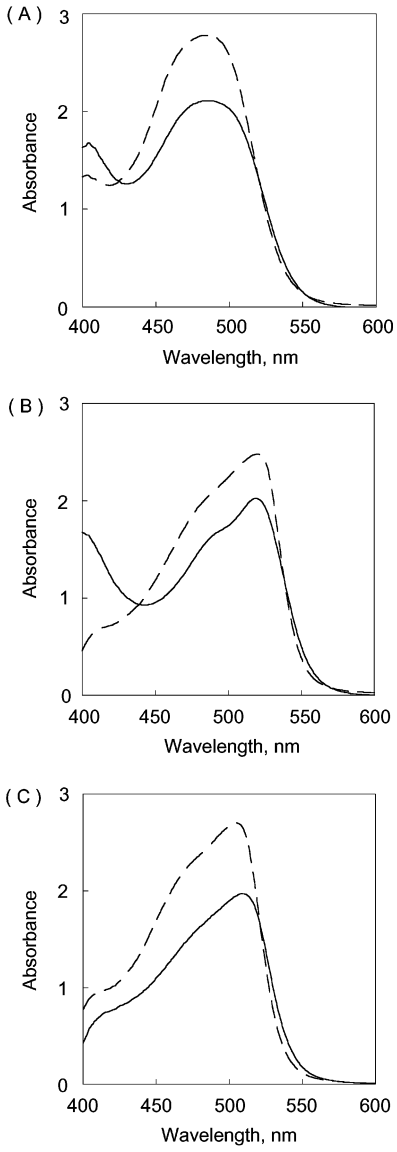

Figure 2. Absorption spectra of (A) OTE/TiO_2/**1** (solid line) and OTE/TiO_2/**4** (dashed line). (B) Absorption spectra of OTE/TiO_2/**2** (solid line) and OTE/TiO_2/**5** (dashed line). (C) Absorption spectra of OTE/TiO_2/**3** (solid line) and OTE/TiO_2/**6** (dashed line).

due to the fluorescence quenching by the photoinduced electron transfer in the DPAX derivatives.[2b] According to the DFT calculations (see Experimental Section), the HOMO and LUMO orbitals of DPAX derivatives are localized on the DPA and X moiety, respectively, as shown in Figure 3 where the calculated results of **2** are given as a representative example.

Photoelectrochemical Properties of DPAX Derivatives on OTE/TiO_2. To evaluate the response of DPAX derivatives toward the photocurrent generation, a series of photocurrent action spectra were recorded. The monochromatic incident photon-to-photocurrent conversion efficiency (IPCE), defined as the number of electrons generated by light in the outer circuit divided by the number of incident photons, was determined by using eq 1:[30]

$$\text{IPCE}\ (\%) = 100 \times 1240 \times I_{sc}(\text{mA/cm}^2)/ [\lambda(\text{nm}) \times P_{in}(\text{mW/cm}^2)] \quad (1)$$

where I_{sc} is the short-circuit photocurrent generated by monochromatic light and λ is the wavelength of incident monochromatic light, whose light intensity is P_{in}.

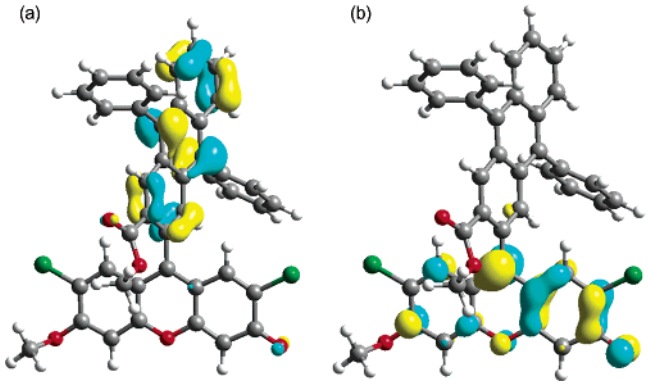

Figure 3. (a) HOMO and (b) LUMO orbitals of ester bodies of **3** calculated by a DFT method with Gaussian 98 (B3LYP/6-31G* basis set).

Figure 4 shows the photocurrent action spectra of DPAX derivatives and the corresponding reference compounds on an OTE/TiO_2 electrode. The IPCE values of the OTE/TiO_2/**1** electrode are larger than those of the OTE/TiO_2/**4** electrode in the visible region. Such enhanced IPCE values in the OTE/TiO_2/**1** electrode relative to the OTE/TiO_2/**4** electrode may be ascribed to the occurrence of efficient charge separation by the photoinduced electron transfer in DPAX **1**. The IPCE values increase in the order: OTE/TiO_2/**1** electrode (maximum IPCE, 12%), OTE/TiO_2/**2** (maximum IPCE, 19%), and OTE/TiO_2/**3** (maximum IPCE, 30%). Such an increase in the IPCE value may result from an increase in the efficiency of charge separation by introducing electron-withdrawing substituents (Cl in **2** and F in **3**) in the xanthene (acceptor) moiety which lower the LUMO level.

The current−voltage (*I-V*) characteristics of DPAX derivatives on OTE/TiO_2 were examined using a thin-layer sandwich-type solar cell under illumination of simulated AM 1.5 solar light (100 mW/cm^2 from a Xe lamp) in order to determine the light-energy conversion efficiency (η). The dye-coated TiO_2 film as working electrode was placed directly on top of an OTE as a counter electrode, on which the Pt was sputtered. The redox electrolyte was introduced into the inter-electrode space by capillary force. The solar cells were illuminated in the front through a conducting glass substrate. Light-energy conversion efficiency, η, is calculated by eq 2,[31]

$$\eta = FF \times I_{sc} \times V_{oc}/P_{in} \quad (2)$$

where the fill factor (*FF*) is defined as $FF = [IV]_{max}/ I_{sc}V_{oc}$, where V_{oc} is the open circuit photovoltage and I_{sc} is the short-circuit photocurrent.

Figure 5 shows the *I-V* characteristics of DPAX derivatives **1**−**3** on OTE/TiO_2. The short-circuit photocurrents (I_{sc}), open-circuit photovoltages, and fill factors (*FF*) are summarized in Table 2, together with the light-energy conversion efficiencies (η), which are determined using eq 2. The η value increases in the order: OTE/TiO_2/**1** (0.38%), OTE/TiO_2/**2** (0.62%), and OTE/TiO_2/**3** (0.85%), in agreement with the order of the IPCE values in Figure 4.

Light−Energy Conversion Properties of DPAX Derivatives on ZnO−SnO_2 Composite Films. Tennakone et al. have reported that DSSCs assembled on ZnO−SnO_2 composite nanoparticles (OTE/ZnO−SnO_2) exhibit more efficient light−energy conversion compared with the corresponding DSSCs on TiO_2 nanoparticles.[24,25] Thus, we examined DSSCs of DPAX derivatives assembled on ZnO−SnO_2 composite nanoparticles in comparison with those on TiO_2. The DSSCs on ZnO−SnO_2

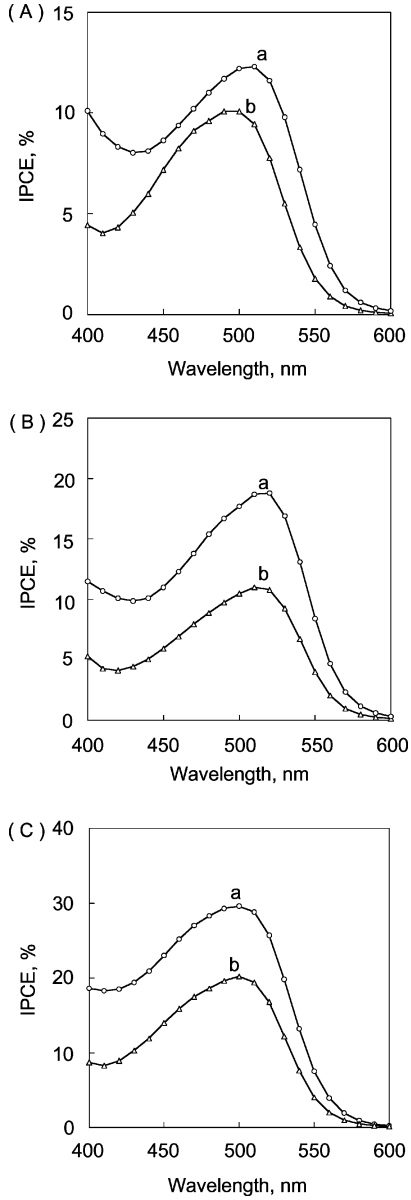

Figure 4. (A) Comparison of photocurrent action spectra (IPCE values) of (a) OTE/TiO_2/**1** with (b) OTE/TiO_2/**4**. (B) Comparison of photocurrent action spectra (IPCE values) of (a) OTE/TiO_2/**2** with (b) OTE/TiO_2/**5**. (C) Comparison of photocurrent action spectra (IPCE values) of (a) OTE/TiO_2/**3** with (b) OTE/TiO_2/**6** electrodes; electrolyte, 0.5 M LiI, 0.05 M I_2, 0.3 M 1,2-dimethyl-3-propylimidazolium iodide, and 0.5 M *tert*-butylpyridine in methoxyacetonitrile.

composite nanoparticles were made by a similar method employed for the preparation of OTE/TiO_2 films.[24,25] The number of adsorbed dye molecules of **1**−**6** on ZnO−SnO_2 films is significantly larger than those of OTE/TiO_2 films (see Table 1).

Figure 6A shows the photocurrent action spectra of OTE/ZnO−SnO_2/**1**, OTE/ZnO−SnO_2/**2**, and OTE/ZnO−SnO_2/**3** electrodes. The IPCE values of DPAX derivatives on the OTE/ZnO−SnO_2 electrodes in Figure 6A are significantly larger than those of the corresponding OTE/TiO_2 electrodes in Figure 4. The IPCE value increases in the order: OTE/ZnO−SnO_2/**1**, OTE/ZnO−SnO_2/**2**, and OTE/ZnO−SnO_2/**3**, in agreement with that of the corresponding OTE/TiO_2 electrodes. The maximum IPCE value reaches 41% in the case of the OTE/ZnO−SnO_2/**3** electrode.

The *I*-*V* characteristics of DPAX derivatives on the OTE/ZnO−SnO_2 electrodes are shown in Figure 6B. The resulting

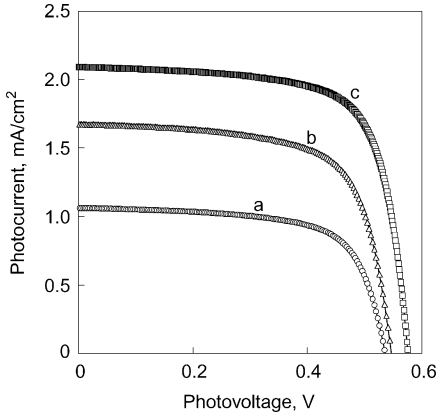

Figure 5. Photocurrent−photovoltage curves of (a) OTE/TiO_2/**1**, (b) OTE/TiO_2/**2**, and (C) OTE/TiO_2/**3** electrodes under white-light illumination; electrolyte, 0.5 M LiI, 0.05 M I_2, 0.3 M 1,2-dimethyl-3-propylimidazolium iodide, and 0.5 M *tert*-butylpyridine in methoxyacetonitrile; input power, 100 mW/cm^2.

TABLE 2: Performance Characteristics of OTE/TiO_2/1, OTE/TiO_2/2, and OTE/TiO_2/3 Electrodes under White-Light Illumination.[a]

	1	**2**	**3**
I_{sc}, mA/cm^2	1.2	1.7	2.1
V_{oc}, mV	540	570	580
FF	0.67	0.68	0.71
η, %	0.38	0.62	0.85
IPCE, % (λ, nm)	12 (510)	19 (520)	30 (500)

[a] Electrolyte, 0.5 M LiI, 0.05 M I_2, 0.3 M 1,2-dimethyl-3-propylimidazolium iodide, and 0.5 M *tert*-butylpyridine in methoxyacetonitrile; input power, 100 mW/cm^2.

data are listed in Table 3. The η values in Table 3 are significantly higher than those in Table 2. Such higher energy conversion efficiencies of the OTE/ZnO−SnO_2 electrodes (Table 3) relative to the corresponding OTE/TiO_2 electrodes (Table 2) largely result from the higher values of I_{sc} and V_{oc} of the OTE/ZnO−SnO_2 electrodes. The large amount of the dye molecules that cover the surface of ZnO−SnO_2 composite film as compared with those on TiO_2 film (Table 1) results in the suppression of the back electron transfer from the dye-covered ZnO−SnO_2 film to I_3^-, leading to an increase in V_{oc} and I_{sc}. The light−energy conversion efficiency (η) in Table 3 increases in the order: OTE/ZnO−SnO_2/**1**, OTE/ZnO−SnO_2/**2**, and OTE/ZnO−SnO_2/**3**. The highest light−energy conversion efficiency (η) is obtained as 1.6% for OTE/ZnO−SnO_2/**3**.[32]

Mechanism of Photocurrent Generation. The photocurrent generation in the fluorescein-sensitized solar cells has previously been reported to be initiated by ultrafast electron injection from the singlet excited state of the fluorecein dye into the conduction band of the semiconductor in the femtosecond time domain.[12,13] In the case of the reference compounds (**4**−**6**), the photoexcitation of the xanthene moiety results in electron injection from the singlet excited state of the dye into the semiconductor conduction band and/or trap states to produce the xanthene radical cation since no electron donor moiety is linked with the xanthene moiety in **4**−**6**. The xanthene moiety has been used as an electron donor in the dyad linked with tris(2,2′-bipyridine)-Ru(II).[33] The photoinduced electron transfer from the xanthene moiety to the excited Ru moiety is thermodynamically allowed.[33,34] The photoinduced electron injection from a xanthene derivative (eosin Y) into the conduction band of TiO_2 has now been well established.[8−13] The resulting xanthene radical cation produced in the photoinduced electron injection to the conduction band of TiO_2 is reduced by the electrolyte ($I_3^-/I^- = 0.5$ V

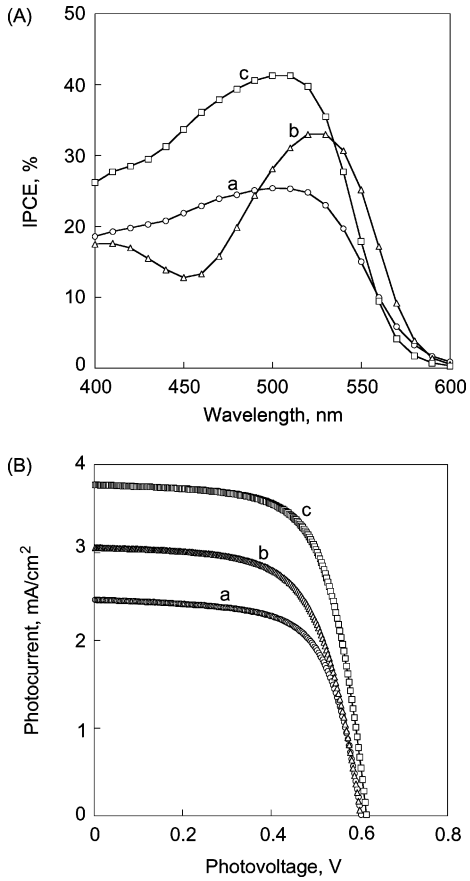

Figure 6. (A) Comparison of photocurrent action spectra (IPCE values) of (a) OTE/ZnO−SnO_2/**1**, (b) OTE/ZnO−SnO_2/**2**, and (c) OTE/ZnO−SnO_2/**3** electrodes. (B) Photocurrent−photovoltage curves of (a) OTE/ZnO−SnO_2/**1**, (b) OTE/ZnO−SnO_2/**2**, and (c) OTE/ZnO−SnO_2/**3** electrodes under white-light illumination; electrolyte, 0.5 M tetrapropylammonium iodide and 0.05 M I_2 in methoxyacetonitrile; input power, 100 mW/cm^2.

TABLE 3: Performance Characteristics of OTE/ZnO−SnO_2/1, OTE/ZnO−SnO_2/2, and OTE/ZnO−SnO_2/3 Electrodes under White-Light Illumination.[a]

	1	**2**	**3**
I_{sc}, mA/cm^2	2.5	3.1	3.8
V_{oc}, mV	610	600	620
FF	0.66	0.64	0.67
η, %	0.98	1.2	1.6
IPCE, % (λ, nm)	25 (510)	33 (520)	41 (500)

[a] 0.5 M Tetrapropylammonium iodide and 0.05 M I_2 in methoxyacetonitrile; input power, 100 MW/cm^2.

vs NHE).[14,35] At the counter electrode, the electron reduces the oxidized electrolyte, I_3^-, leading to photocurrent generation.

In the case of DPAX, the donor (DPA) moiety, which is linked with the xanthene moiety, is adsorbed on the semiconductor surface with the carboxylate group, as shown in Scheme 1 where the structure of DPAX is optimized by the DFT calculation (see Experimental Section). In this case, the xanthene radical cation produced in the photoinduced electron injection from the singlet excited state of the xanthene dye to the conduction band of TiO_2 may be efficiently reduced by the donor (DPA) moiety via intramolecular electron transfer rather than by the electrolyte (I_3^-/I^- = 0.5 V vs NHE) via intermolecular electron transfer (Scheme 1).[36] The resulting $DPA^{\bullet+}$ is reduced by the electrolyte (I_3^-/I^- = 0.5 V vs NHE) to regenerate DPA.[14,35] The electron is collected at the back contact to perform electrical work in the external circuit. At the counter

SCHEME 1: The Optimized Structure of OTE/Semiconductor/1 Calculated by a DFT Method with B3LYP/6-31G*

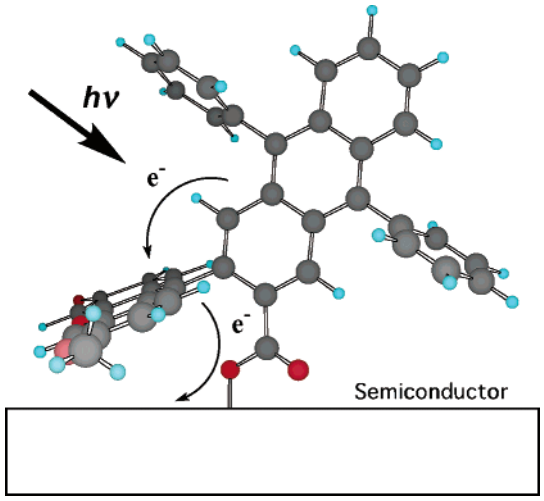

electrode, the electron reduces the electrolyte, I_3^-. Alternatively, the singlet excited state of the xanthene moiety is also quenched by the electron transfer from the donor (DPA) moiety. The occurrence of such photoinduced electron transfer has been firmly established by the direct detection of the radical cation of the donor (DPA) moiety and the radical anion of the acceptor (xanthene) moiety in the laser flash photolysis experiments.[5] In such a case, the xanthene moiety can also act as an electron acceptor rather than as an electron donor, in contrast with the case of fluorescein derivatives without a donor moiety. Since the xanthene moiety is located in close proximity to the semiconductor surface (Scheme 1) and the redox potential of xanthene/xanthene$^{\bullet-}$ (−1.0 V vs NHE)[5] is lower than that of the conduction band (−0.5 V vs NHE),[14,35] the resulting xanthene radical anion can inject an electron to the conduction band of the semiconductor. In any case, $DPA^{\bullet+}$ remains after the electron injection, being reduced by the electrolyte (I_3^-/I^- = 0.5 V vs NHE) to regenerate DPA.[14,35]

Conclusion

We have constructed dye-sensitized solar cells (DSSC) based on 9-[2-(3-carboxy-9,10-diphenyl)anthryl]-6-hydroxy-3*H*-xanthen-3-one (DPAX) derivatives (**1**−**3**) containing an electron donor moiety (diphenylanthracene), which exhibit higher IPCE and η values than those of the corresponding reference compounds (**4**−**6**) without charge separation. This indicates that the xanthene derivatives linked with an electron donor moiety act as superior dyes for efficient light−energy conversion compared with the reference dyes without an electron donor moiety, which undergo direct photoinduced electron injection into the conduction band of TiO_2. The light−energy conversion efficiency (η) increases by introducing electron-withdrawing substituents (Cl in **2** and F in **3**) in the xanthene (acceptor) moiety, and the highest light−energy conversion efficiency (η = 1.6%) is attained for OTE/ZnO−SnO_2/**3**. Lowering the LUMO level by introducing electron-withdrawing substituents may facilitate the photoinduced charge separation in competition with the energy transfer to produce the triplet excited sate of xanthene, leading to the more efficient light−energy conversion. Although the power-conversion efficiency of the charge-separation-type DSSC is still lower than that of typical inorganic solar cells, easy chemical modification of the charge-separation-type organic dyads, as compared with inorganic solar cells, provides the bright future prospect of developing more efficient DSSC.

Acknowledgment. This work was partially supported by a grant in aid (13440216) from the Ministry of Education, Culture, Sports, Science and Technology, Japan. We are grateful to Dr. Takayuki Kitamura, Osaka University, for helping with the preparation of the DSSC.

Supporting Information Available: Absorption spectra of **1**−**6** (S1), the spectral and redox potential data of **1**−**3** (S2), and plot of I_{sc} vs light intensity (S3). This material is available free of charge via the Internet at http://pubs.acs.org.

References and Notes

(1) Minta, A.; Kao, J. P. Y.; Tsien, R. Y. *J. Biol. Chem.* **1989**, *264*, 8171.

(2) (a) Kojima, H.; Nakatsubo, N.; Kikuchi, K.; Kawahara, S.; Kirino, Y.; Nagoshi, H.; Hirata, Y.; Nagano, T. *Anal. Chem.* **1998**, *70*, 2446. (b) Umezawa, N.; Tanaka, K.; Urano, Y.; Kikuchi, K.; Higuchi, T.; Nagano, T. *Angew. Chem., Int. Ed.* **1999**, *38*, 2899.

(3) Walkup, G. K.; Burdette, S. C.; Lippard, S. J.; Tsien, R. Y. *J. Am. Chem. Soc.* **2000**, *122*, 5644.

(4) (a) Hirano, T.; Kikuchi, K.; Urano, Y.; Higuchi, T.; Nagano, T. *J. Am. Chem. Soc.* **2000**, *122*, 12399. (b) Tanaka, K.; Miura, T.; Umezawa, N.; Urano, Y.; Kikuchi, K.; Higuchi, T.; Nagano, T. *J. Am. Chem. Soc.* **2001**, *123*, 2530.

(5) Miura, T.; Urano, Y.; Tanaka, K.; Nagano, T.; Ohkubo, K.; Fukuzumi, S. *J. Am. Chem. Soc.* **2003**, *125*, 8666.

(6) Kamat, P. V.; Fox, M. A. *Chem. Phys. Lett.* **1983**, *102*, 379.

(7) Rossetti, R.; Brus, L. E. *J. Am. Chem. Soc.* **1984**, *106*, 4336.

(8) (a) Moser, J.; Grätzel, M. *J. Am. Chem. Soc.* **1984**, *106*, 6557. (b) Moser, J.; Grätzel, M.; Sharma, D. K.; Serpone, N. *Helv. Chim. Acta* **1985**, *68*, 1686.

(9) Benkö, G.; Hilgendorff, M.; Yartsev, A. P.; Sundström, V. *J. Phys. Chem. B* **2001**, *105*, 967.

(10) (a) Hilgendorff, M.; Sundström, V. *Chem. Phys. Lett.* **1998**, *287*, 709. (b) Hilgendorff, M.; Sundström, V. *J. Phys. Chem. B* **1998**, *102*, 10505.

(11) Walters, K. A.; Gaal, D. A.; Hupp, J. T. *J. Phys. Chem. B* **2002**, *106*, 5139.

(12) Benkö, G.; Skårman, B.; Wallenberg, R.; Hagfeldt, A.; Sundström, V.; Yartsev, A. P. *J. Phys. Chem. B* **2003**, *107*, 1370.

(13) Pelet, S.; Grätzel, M.; Moser, J.-E. *J. Phys. Chem. B* **2003**, *107*, 3215.

(14) For dye-sensitized organic solar cells, see: (a) Hagfeldt, A.; Grätzel, M. *Chem. Rev.* **1995**, *95*, 49. (b) Hagfeldt, A.; Grätzel, M. *Acc. Chem. Res.* **2000**, *33*, 269.

(15) *The Photosynthetic Reaction Center*; Deisenhofer, J., Norris, J. R., Eds.; Academic Press: San Diego, 1993.

(16) (a) Gust, D.; Moore, T. A.; Moore, A. L. *Acc. Chem. Res.* **1993**, *26*, 198. (b) Gust, D.; Moore, T. A.; Moore, A. L. In *Electron Transfer in Chemistry*, Balzani, V., Ed.; Wiley-VCH: Weinheim, 2001; Vol. 3, pp 272−336.

(17) (a) Wasielewski, M. R. *Chem. Rev.* **1992**, *92*, 435. (b) Osuka, A.; Mataga, N.; Okada, T. *Pure Appl. Chem.* **1997**, *69*, 797.

(18) (a) Jordan, K. D.; Paddon-Row: M. N. *Chem. Rev.* **1992**, *92*, 395. (b) Paddon-Row, M. N. *Acc. Chem. Res.* **1994**, *27*, 18. (c) Paddon-Row, M. N. *Adv. Phys. Org. Chem.* **2003**, *38*, 1.

(19) (a) Verhoeven, J. W. *Adv. Chem. Phys.* **1999**, *106*, 603. (b) Verhoeven, J. W. In *Electron Transfer-From Isolated Molecules to Biomolecules*; Jortner, J., Bixon, M., Eds.; John Wiley & Sons: New York, 1999; Part 1, pp 603−644.

(20) (a) Harriman, A.; Sauvage, J.-P. *Chem. Soc. Rev.* **1996**, *25*, 41. (b) Blanco, M.-J.; Jiménez, M. C.; Chambron, J.-C.; Heitz, V.; Linke, M.; Sauvage, J.-P. *Chem. Soc. Rev.* **1999**, *28*, 293.

(21) (a) Fukuzumi, S.; Guldi, D. M. In *Electron Transfer in Chemistry*; Balzani, V., Ed.; Wiley-VCH: Weinheim, 2001; Vol. 2, pp 270−337. (b) Fukuzumi, S. *Org. Biomol. Chem.* **2003**, *1*, 609.

(22) (a) Fukuzumi, S.; Ohkubo, K.; Imahori, H.; Shao, J.; Ou, Z.; Zheng, G.; Chen, Y.; Pandey, R. K.; Fujitsuka, M.; Ito, O.; Kadish, K. M. *J. Am. Chem. Soc.* **2001**, *123*, 10676. (b) Kashiwagi, Y.; Ohkubo, K.; McDonald, J. A.; Blake, I. M.; Crossley, M. J.; Araki, Y.; Ito, O.; Imahori, H.; Fukuzumi, S. *Org. Lett.* **2003**, *5*, 2719.

(23) (a) Ohkubo, K.; Kotani, H.; Shao, J.; Ou, Z.; Kadish, K. M.; Li, G.; Pandey, R. K.; Fujitsuka, M.; Ito, O.; Imahori, H.; Fukuzumi, S. *Angew. Chem., Int. Ed.* **2004**, *43*, 853. (b) Fukuzumi, S.; Kotani, H.; Ohkubo, K.; Ogo, S.; Tkachenko, N. V.; Lemmetyinen, H. *J. Am. Chem. Soc.* **2004**, *126*, 1600.

(24) (a) Tennakone, K.; Kumara, G. R. R. A.; Kottegoda, I. R. M.; Perera, V. P. S. *J. Chem. Commun.* **1999**, 15. (b) Tennakone, K.; Kottegoda, I. R. M.; De Silva, L. A. A.; Perera, V. P. S. *Semicond. Sci. Technol.* **1999**, *14*, 975.

(25) Kumara, G. R. R. A.; Konno, A.; Tennakone, K. *Chem. Lett.* **2001**, 180.

(26) (a) Becke, A. D. *J. Chem. Phys.* **1993**, *98*, 5648. (b) Lee, C.; Yang, W.; Parr, R. G. *Phys. Rev. B* **1988**, *37*, 785.

(27) Hehre, W. J.; Radom, L.; Schleyer, P. v. R.; Pople, J. A. *Ab Initio Molecular Orbital Theory*; Wiley: New York, 1986.

(28) Frisch, M. J.; Trucks, G. W.; Schlegel, H. B.; Scuseria, G. E.; Robb, M. A.; Cheeseman, J. R.; Zakrzewski, V. G.; Montgomery, J. A., Jr.; Stratmann, R. E.; Burant, J. C.; Dapprich, S.; Millam, J. M.; Daniels, A. D.; Kudin, K. N.; Strain, M. C.; Farkas, O.; Tomasi, J.; Barone, V.; Cossi, M.; Cammi, R.; Mennucci, B.; Pomelli, C.; Adamo, C.; Clifford, S.; Ochterski, J.; Petersson, G. A.; Ayala, P. Y.; Cui, Q.; Morokuma, K.; Malick, D. K.; Rabuck, A. D.; Raghavachari, K.; Foresman, J. B.; Cioslowski, J.; Ortiz, J. V.; Baboul, A. G.; Stefanov, B. B.; Liu, G.; Liashenko, A.; Piskorz, P.; Komaromi, I.; Gomperts, R.; Martin, R. L.; Fox, D. J.; Keith, T.; Al-Laham, M. A.; Peng, C. Y.; Nanayakkara, A.; Gonzalez, C.; Challacombe, M.; Gill, P. M. W.; Johnson, B.; Chen, W.; Wong, M. W.; Andres, J. L.; Gonzalez, C.; Head-Gordon, M.; Replogle, E. S.; Pople, J. A. *Gaussian 98*, revision A.7; Gaussian, Inc.: Pittsburgh, PA, 1998.

(29) The molar absorption coefficients (ϵ) of DPAX derivatives **1**−**3** and reference compounds **4**−**6** are 9.1×10^4, 9.2×10^4, 9.3×10^4, 9.2×10^4, 9.3×10^4, and 9.3×10^4 $M^{-1}cm^{-1}$, respectively.

(30) Khazraji, A. C.; Hotchandani, S.; Das, S.; Kamat, P. V. *J. Phys. Chem. B* **1999**, *103*, 4693.

(31) (a) Kamat, P. V.; Barazzouk, S.; Thomas, K. G.; Hotchandani, S. *J. Phys. Chem. B* **2000**, *104*, 4014. (b) Sudeep, P. K.; Ipe, B. I.; Thomas, K. G.; George, M. V.; Barazzouk, S.; Hotchandani, S.; Kamat, P. V. *Nano Lett.* **2002**, *2*, 29. (c) Kamat, P. V.; Barazzouk, S.; Hotchandani, S. Thomas, K. G. *Chem. Eur. J.* **2000**, *6*, 3914.

(32) The I_{SC} value is proportional to the light intensity (see Supporting Information, S3).

(33) Jing, B.; Zhang, M.; Shen, T. *Org. Lett.* **2003**, *5*, 3709.

(34) Yu, Q.; He, J.; Shen, T. *J. Photochem. Photobiol. A* **1996**, *97*, 53.

(35) (a) Hasobe, T.; Imahori, H.; Fukuzumi, S.; Kamat, P. V. *J. Mater. Chem.* **2003**, *13*, 2515. (b) Hasobe, T.; Imahori, H.; Fukuzumi, S.; Kamat, P. V. *J. Phys. Chem. B* **2003**, *107*, 12105.

(36) For dye-sensitized solar cells using donor−acceptor type sensitizers, see: (a) Bonhôte, P.; Moser, J.-E.; Humphry-Baker, R.; Vlachopoulos, N.; Zakeeruddin, S. M.; Walder, L.; Grätzel, M. *J. Am. Chem. Soc.* **1999**, *121*, 1324. (b) Argazzi, R.; Bignozzi, C. A.; Heimer, T. A.; Castellano, F. N.; Meyer, G. J. *J. Phys. Chem. B* **1997**, *101*, 2591.